GREENLAND ICE SHEET CLIMATOLOGY AND SURFACE ENERGY BALANCE MODELING: Greenland Climate Network (GC-Net)

K. Steffen and J. Box
University of Colorado at Boulder
Cooperative Institute for Research in Environmental Sciences
Division of Cryospheric and Polar Processes
Campus Box 216, Boulder CO 80309

NAGW-4248
Progress Report
to
National Aeronautics and Space Administration

December 1998

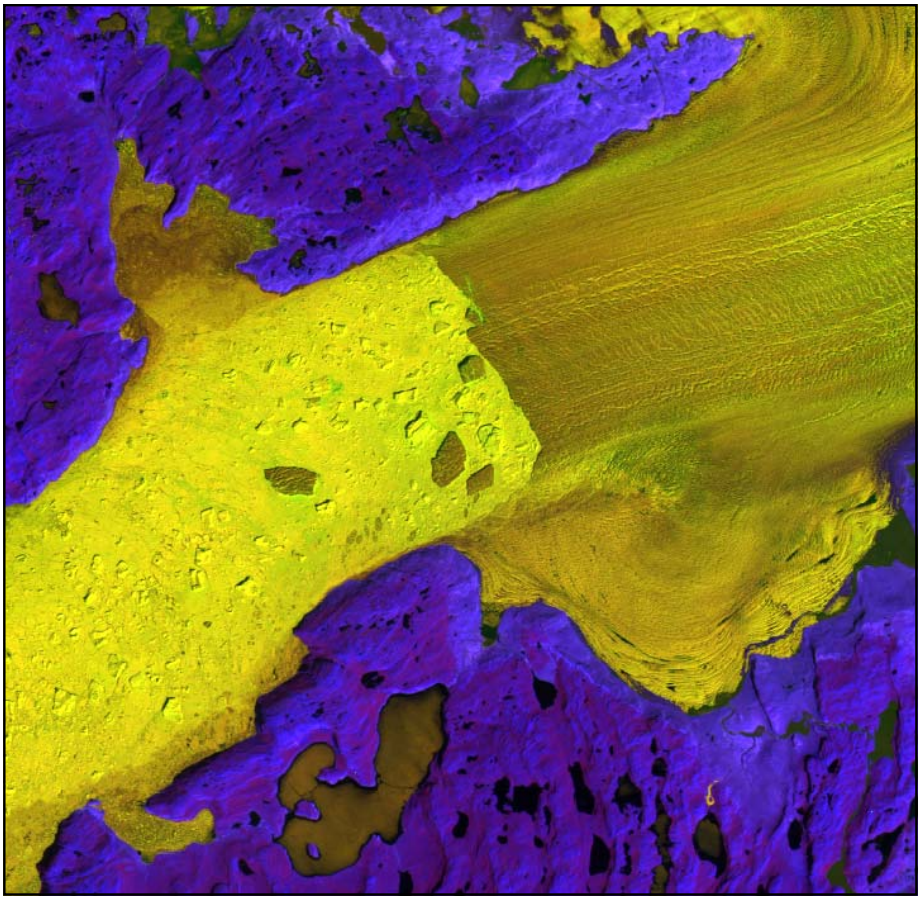

JAKOBSHAVN GLACIER (LANDSAT TM IMAGE, 22 JUNE 1990)

TABLE OF CONTENTS

Summery of Highlights

Greenland Climate Network

- One new automatic weather station (NASA-SE) has been installed during the '98 field season to increase the GC-Net to a total of 15 stations.
- Eleven AWS maintenance jobs were carried out at Swiss Camp, JAR, Crawford Point-1, Crawford Point-2, Summit, DYE2, GITS, NASA-U, S-Dome, NGRIP and Saddle.
- A complete annual GPS record was recovered from the Swiss Camp, with weekly measurements covering the time period June 97 to May 98. The Trimble 4000SSE instruments was powered by solar panels connected to four 100 Ah batteries.
- A total of twenty-eight station years of GC-Net measurements has been processed and is available for the general science community.
- GC-Net data set has been calibrated and annual, monthly and daily averages are now available. A linear regression was done for each AWS mean-monthly AWS parameter and for every station. The correlation between the stations was sufficiently high that the empirical regression could be used to fill-in missing monthly data.

Greenland Ice Sheet Climatology

- A linear regression to estimate annual rate of surface height change at 12 AWS explained between 91 and 99% of the hourly variance.
- The continuous climate record at the Swiss Camp (since April 1991 to present) is the longest meteorological record on the Greenland ice sheet. The mean annual air temperature has increased by 1° C per year, from -16° to -11° C between 1992 and 1997.
- Monthly mean latent heat flux was calculated based on the aerodynamic profile method for several AWS stations. For the Swiss Camp, the monthly values are negative, ranging between 0 to -80 W m^{-2}, which corresponds to mass loss of 0 to -70 kg m^{-2} per month.
- Blowing snow is important to local-scale mass balance even while mass loss off the ice-sheet edge is small. Largest mass fluxes were found at the lower elevations of the Greenland ice sheet due to increased katabatic wind speeds at low elevations. Values range from 0 10^{12} g km^{-1} yr^{-1} at high elevations to 5 10^{12} g km^{-1} yr^{-1} along the coast.
- UV radiation under clouds was found to be enhanced by 100% as compared to total radiation. For mid-latitudes this ratio is only 1.2, or 20%.
- Faceted snow crystals were found under wind crusts at the Tunu-N location. Snow and air temperatures from the Tunu-N AWS suggest that the katabatic storms are responsible for the wind crust and the faceted layers.
- A total of 13 papers has been published or is in press in peer-reviewed journals supported by this grant.

1. Introduction

1.1 Rational of the Study

Climatological observations and surface energy balance studies are the keys to the understanding of the surface processes linked with ice sheet mass balance. Long-term climate records at different sites on the ice sheet are needed for the assessment of the snow pack energy and mass balance of the accumulation zone and to gain more complete information of the spatial variation of climate over the ice sheet. A considerable amount of surface energy and mass balance data as well as some ice cores have been collected at the ETH/CU research camp since 1990. The camp is located at the ice sheet equilibrium line altitude (ELA), about 89 km east of Jakobshavn at 69° 34' N, 49° 17' W on the western margin of the Greenland ice sheet (Fig. 1.1). Seven years of detailed climatological and glaciological measurements at the camp provide valuable insight on the magnitude of the seasonal and interannual variability in the equilibrium zone. Based on the ETH/CU camp energy flux measurements, a simple climate sensitivity model calculation showed, that during a 3° C temperature increase scenario, approximately 22 km^3 water equivalent of snow would sublimate. This equals 4% of today's annual accumulation. Large seasonal and interannual variations in air temperature and wind speed were found for the location of the ETH/CU camp based on the seven year record. Surface temperature anomalies in the order of -3° C along the west coast of Greenland for the winter months have also been reported since 1990. In contrast, a notable increasing trend of 4.5% per year in melt area has been observed between the years 1979-91, which came to an abrupt halt in 1992 after the eruption of Mt. Pinatubo. A similar trend is observed in the temperatures at six coastal stations.

The Greenland Climate Network (GC-Net) was established in spring 1994 with the emphasis to monitor climatological and glaciological parameters at various locations on the ice sheet over a time period of at least 5 years. The objectives of the GC-Net automatic weather station (AWS) network are:

- Assess daily, annual and interannual variability in accumulation rate, surface climatology and surface energy balance at selected locations on the ice sheet where high sensitivity of the ice sheet mass balance to climate anomalies is predicted from modeling results.
- Assess accurate surface elevation, location, near-surface density at the AWS location with the option to revisit the locations in order to get temporal information for dynamic ice sheet modeling.
- The objective of this study is to model the surface energy balance based on atmospheric and cyrospheric interactions, using the Greenland climate network of AWS stations as input parameters. In a first attempt, the surface energy balance of the western part of the ice sheet will be modeled, using the current AWS network.

Another important factor is the surface orography. The surface topography with scale length of several kilometers plays an important role for the spatial variability of accumulation. The knowledge of this surface roughness is essential for the spatial surface energy balance modeling. One of the major applications of ice core data is the estimation of snow accumulation in the vicinity of the core location. A major problem arises however in identification of the date of peak isotope. A one month underestimation in one year followed by a one month overestimation in another, results in a time error of 17%. Such an error significantly alters the estimated annual accumulation rates. Using a combination of different passive microwave frequencies with their varying penetration depths, estimates of the date of maximum and minimum surface temperatures can be made as a function of the brightness temperature characteristics. These minimum temperature estimates can be correlated with air temperatures recorded by existing AWS.

1.2 Logistic Summary '98

Eleven AWS maintenance jobs were carried out at Swiss Camp, JAR, Crawford Point-1, Crawford Point-2, Summit, DYE2, GITS, and NASA-U. The new AWS at TUNU-S was postponed to the 1999 field season due to logistics. We retrieved data from the Trimble 4000SSE GPS instrument at the ETH/CU camp, which recorded once a week for a few hours from June 97 to May 98.

Name	*Institution*	*Arr.*	*Dep.*
Jason Box	CU-Boulder	4/18	6/6
Konrad Steffen	CU-Boulder	5/14	6/10
Karen Lewis	CU-Boulder	5/14	6/14
Jeff Weber	CU-Boulder	4/18	4/28
Waleed Abdalati	NASA-GSFC	5/26	6/6
Jay Zwally	GSFC-NASA	5/14	5/21

Date	**Location**	**Work**
4/14-18	SFJ	Organization for AWS maintenance trips.
4/18 – 6/6	divers sites	AWS maintenance 11 stations
5/14	SFJ - Swiss Camp	Opening camp, two flights
5/19	Swiss Camp – JAV	Air Alpha emergency flight (Jay Zwally)
5/19	JAV – SFJ	Zwally on GreenlandAir to Sondy with broken ribs
6/6	Swiss Camp – JAV	Pull-out Swiss Camp with GreenlandAir S61 helicopter
6/6	JAV – SFJ	Flight to Sondy with equipment on GreenlandAir
6/9	SFJ – NGRIP	AWS maintenance, flight on C-130, Steffen and Lewis
6/10	NGRIP – SFJ	Return to Sondy (Steffen) on C-130
6/13	NGRIP – SFJ	Return to Sondy (Lewis) on C-130

2.0 GC-Net Status

During the 1998 field season, 11 of 15 AWS were visited for maintenance and calibration. The AWS team was on the ice cap April 18th through June 6th with 25 field days devoted to AWS work. AWS datasets collected in the field during the 1998 field season have replaced those transmitted datasets. The GC-Net archive has been brought up to date with a single common format for all station data. Compared with last year's 17 station years, there are now 28 station years of GC-Net measurements processed and available for use.

The ARGOS satellite data retrieval now updates automatically. Other steps in the data processing system have been refined and/or automated. The quality control procedures have been refined. More comprehensive documentation is available on station data sets. An HTML-based file server is in operational use internally.

We experienced one station failure at Crawford Pt. (CP1) on Julian day 309 1997. CP1 was reactivated day 150 1998. Fortunately, the Crawford Point 2 (CP2) station was running while CP 1 was out. CP 2 is 6 km from CP 1. Regression between the overlap of CP1 and CP 2 data was established to reconstruct the missing CP1 data. No other station failures occurred unless unknown failures have occurred at stations where we don't have up to date transmissions.

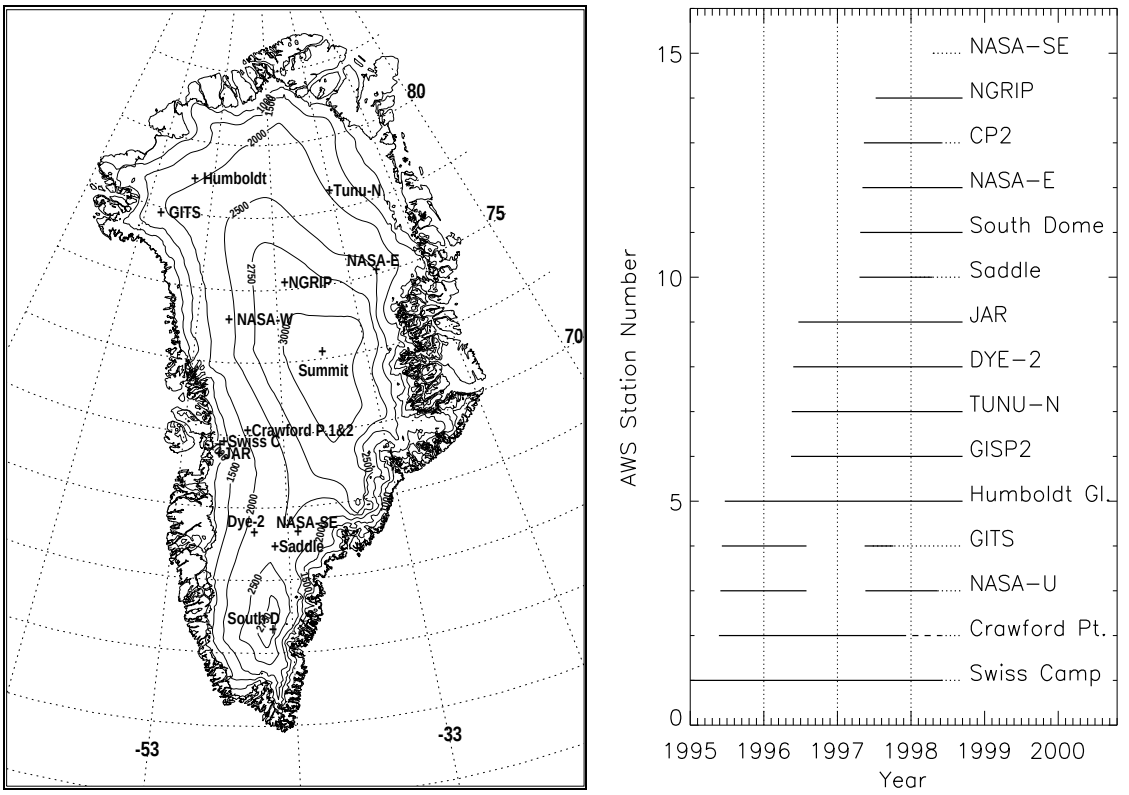

Figure 2.1: GC-Net timeline on the right. The dotted line represents uncertain AWS status due to no satellite data link. The dashed line represents reconstructed Crawford Pt. data. The distribution of automatic weather stations on the Greenland ice sheet (left Figure), as part of the Program for Arctic Regional Climate Assessment (PARCA) Greenland Climate Network (GC-Net).

2.1 Quality Control Advances

Knowledge of whether quality control procedures have been applied to the AWS data is important for data users. An identifier code has been included with each AWS data set to allow the user to identify whether a given hourly data point has been synthesized, as in the case for interpolation, and which filter rejected the data point in question. Synthetic values comprise between 1% and 10% of the entire data volume by station.

2.2 Annual, Monthly, and Daily Averages now Available

AWS data have been averaged on annual, monthly, and daily time-scales. Annual averages have been set to rely on at least 90% of one year. Daily averages rely upon a 95% available data threshold. Three levels of monthly means are now available. One level is based upon a 95% available data threshold (in other words, at least 95% of the available hourly measurements are required for a mean value to be output). A less conservative 90% (availability) monthly data product is also available. A third data set called "reconstructed" provides monthly mean values at the 90% level with data gaps reconstructed (see next paragraph).

2.3 Regression Reconstruction

A linear regression was done for each AWS mean-monthly AWS parameter and for every station. For many of the parameters the explained variance between stations was sufficiently high that the empirical regression could be used to fill in missing monthly data. The third level of monthly mean data available includes the 'real' measurements as well as simulated monthly mean data based upon the empirical regression between all GC-Net stations that qualify above a conservative significance threshold. The simulated values allow a more continuous monthly time series where the available measurements did not pass the 90% available data thresholds as well as an extension of available records beyond their duration's at that site. For example, the explained variance in monthly mean air temperature between DYE-2 and Saddle is 99.8%. DYE-2 AWS has been measuring for 1 year more than Saddle. Hence, where DYE-2 data are available, the empirical function can be used to construct a time series for the Saddle AWS when it was not in operation. Another threshold of at least 10 months is required for the regression to be able to fill in data gaps.

The main purpose, however, is to fill in data gaps where station measurements did not pass quality control procedures more than 90% of the time each month. A significance threshold was set for each parameter, for example air temperature, an explained variance of 95% is required, for wind speed and 85% threshold was assigned, for relative humidity 90% was required.

2.4 Data Availability

To construct a list of data users, we will distribute GC-Net data on a request basis only. Send us email with your request (jbox@ice.colorado.edu or koni@seaice.colorado.edu) and we will provide the data in a timely manner.

3.0 Results

3.1 Estimating Surface Height Change from Sonic Height Measurements

Linear regression was used to estimate annual rate of surface height change at each of the 12 AWS's. At accumulation zone AWS sites, the linear model explained between 91 and 99 % of the hourly variance. Low fit-quality is observed at lower elevations due to ablation. Linear fit residuals allow for calculation of error/variance for surface height changes derived by the sonic instruments.

Table 3.1: Annual Surface Height Change Statistics

AWS	dh/da 1 [m yr^{-1}]	dh/da 2 [m yr^{-1}]	r^2 1	r^2 2	Years 1	years 2	std.1 [m]	std.2 [m]
Sw. Camp	0.12	0.1	0.62	0.6	1.93	1.93	0.3	0.3
Cr. Pt.1	1.34	1.24	0.98	0.89	3.02	3.02	0.17	0.39
NASA-U	1.18	1.16	0.96	0.96	2.15	2.15	0.08	0.08
GITS	1.32	1.14	0.99	0.91	1.68	0.78	0.08	0.08
Humb.	0.47	0.48	0.98	0.97	3.23	3.23	0.06	0.07
Summit	0.63	0.62	0.99	0.99	2.32	2.32	0.05	0.05
TUNU-N	0.42	0.37	0.96	0.96	2.34	2.34	0.05	0.05
DYE-2	0.91	0.91	0.98	0.98	2.31	2.31	0.09	0.08
JAR	-0.37	-7.24	0.18	0.90	2.24	0.31	0.52	0.22
Saddle	1.24	1.29	0.96	0.96	0.99	0.99	0.07	0.07
S Dome	1.86	1.86	0.97	0.97	1.39	1.39	0.14	0.14
NASA-E	0.38	0.42	0.92	0.95	1.37	1.37	0.04	0.04
Cr. Pt. 2	1.69	1.66	0.94	0.95	1.05	1.05	0.13	0.12
NGRIP	0.5	. 7090.96	0.96	0.97	1.19	1.19	0.04	0.03

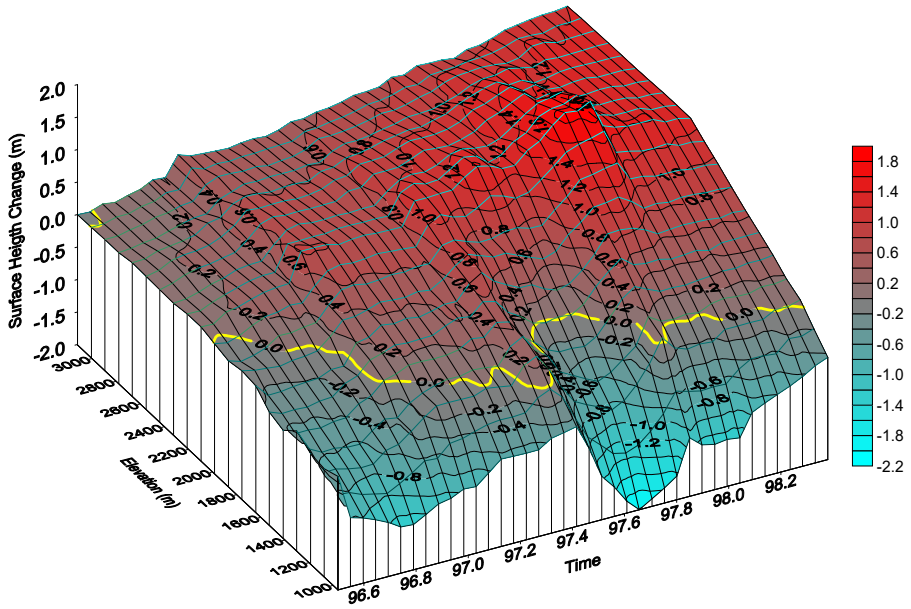

Figure 3.1: Surface height change from July 1996 through March 1998 along the elevation profile JAR – Swiss Camp – Crawford Point 1 – Summit measured with the sonic height sensors.

Monthly surface height changes for 14 GC-Net stations are featured below. Pronounced summer ablation is evident at the Swiss Camp (1150 m) and at JAR (960 m). A springtime minimum is observed at Humboldt, and a minimum is observed during summer at Saddle. Deflation will minimize the accumulation signal.

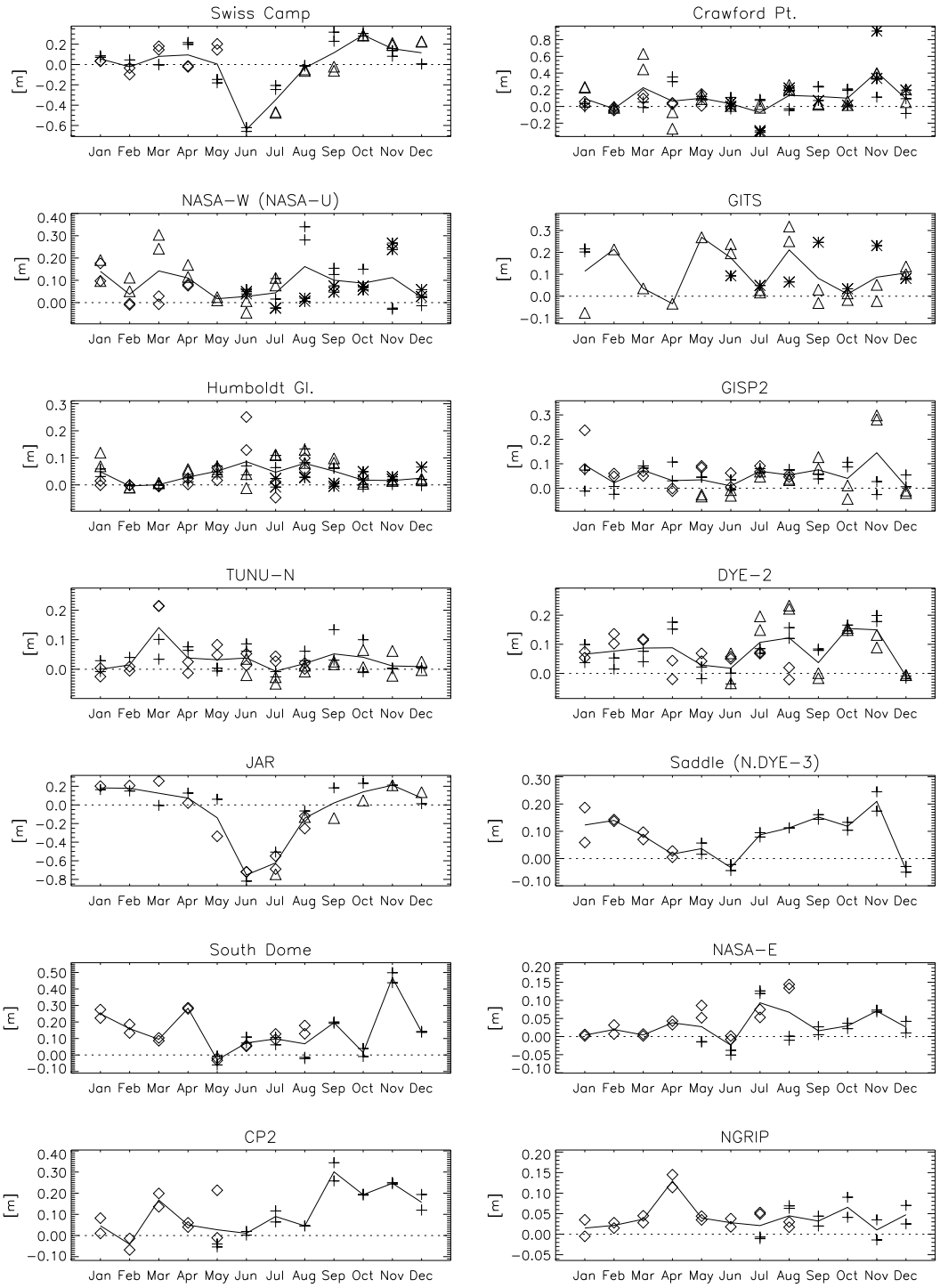

*Figure 3.2: Monthly mean surface height change: * - 1995, Δ - 1996, + 1997, ◊ 1998, ___ - average.*

3.2 Climate Variations at the Swiss Camp: 1991-1998

The continuous climate record at the Swiss Camp (since April 1991 to present) is the longest meteorological record on the Greenland ice sheet. The monthly mean air temperatures are shown in Figure 3.3. The interannual variability of air temperatures is large, with decreasing annual amplitudes towards present. The mean annual air temperature has increased by 1° C per year, from -16° to -11° C between 1992 and 1997. The highest summer temperatures were recorded for the month of July, with no clear summertime trend over the seven years. This is not surprising, since the air temperatures cannot increase significantly above 0° C over a snow/ice surface. Summer temperatures were below normal for 1991 and 1992 due to the cooling effect of the aerosol loading in the stratosphere induced by the Mt. Pinatubo eruption. The coldest winter temperatures were recorded for the month of March, with a significant increase in springtime temperatures between 1993 and 1996. The winter temperatures showed the interannual strongest fluctuations, with a mean increase of 1.2° C/a for February and 0.6° C/a for the month of March.

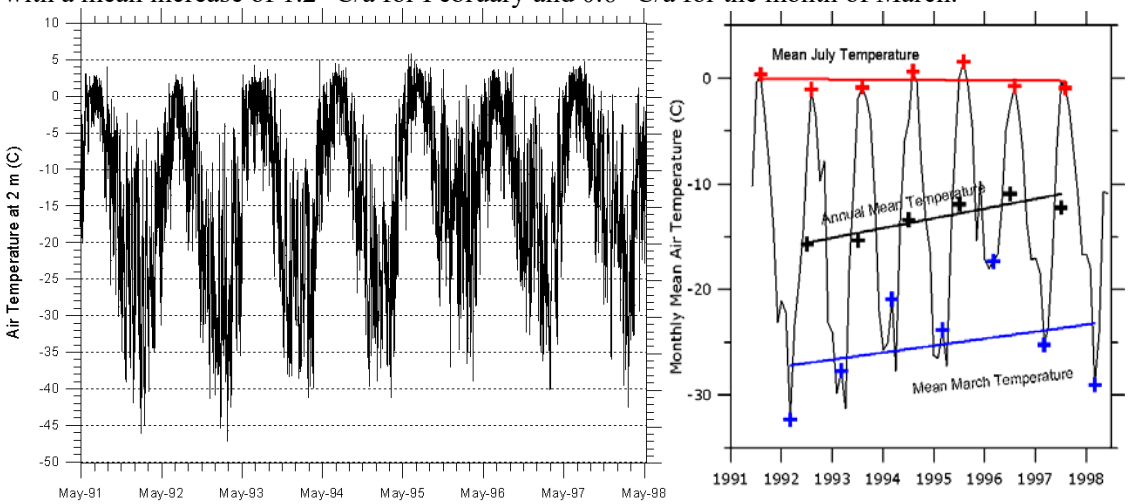

Figure 3.3: Hourly and mean monthly air temperatures for the Swiss Camp (ETH/CU AWS) for 1991-1998. A linear regression line is shown for the July mean temperature, March mean temperature and annual mean temperature.

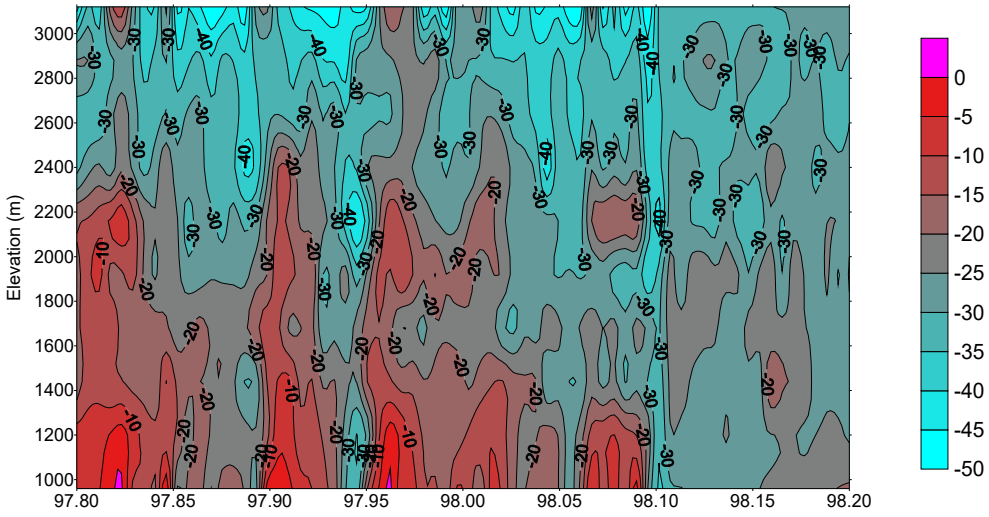

Figure 3.4: Forcing of the surface air temperature along the profile JAR – Swiss Camp – Crawford Point – Summit due to katabatic winds during winter 1997-98.

3.3 Evaporative Mass Fluxes

The latent heat flux was calculated using GC-Net measurements. The aerodynamic profile method was employed, using vertical gradients of moisture, heat, and momentum. The monthly averages are realistic despite large variance (Fig. 3.5).

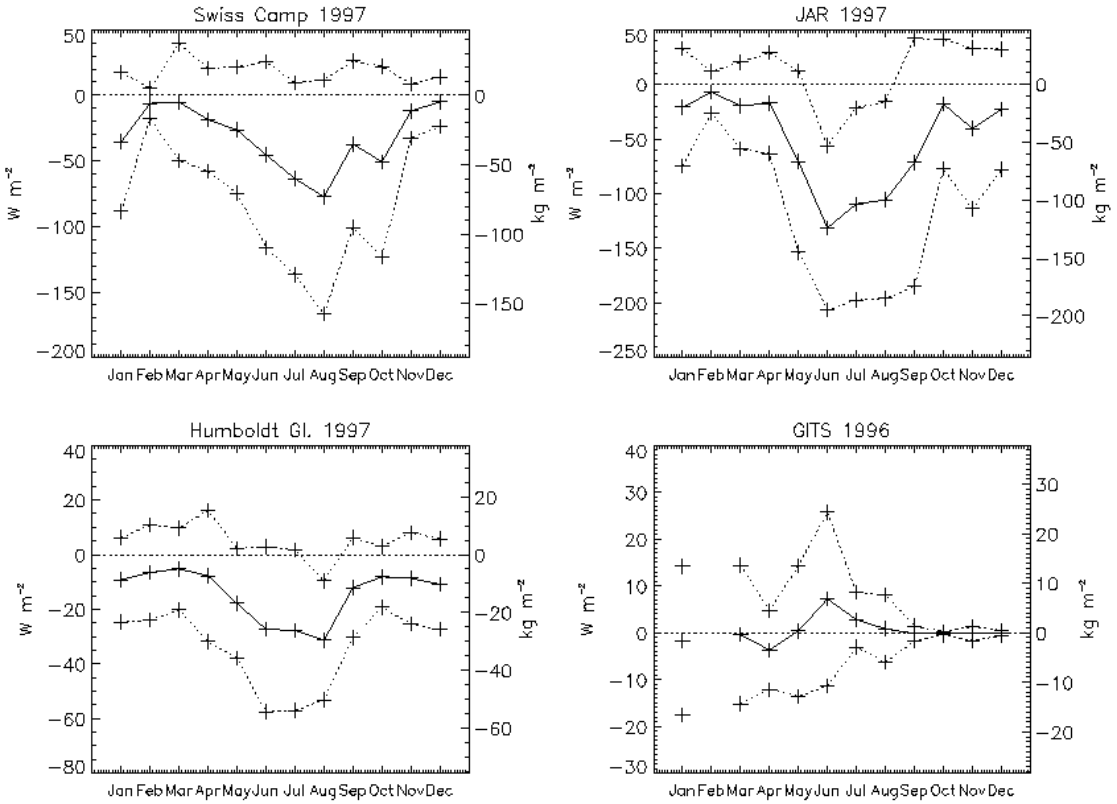

Figure 3.5: Example of one annual cycle of monthly mean latent heat fluxes (left axis) *and corresponding monthly evaporative mass transfers* (right axis) *with ± 1 standard deviation based upon hourly observations.*

On a monthly and annual basis, the latent heat fluxes are typically negative indicating net mass loss by sublimation. Larger sublimation losses occur during summer months when there is likely to be a surplus of radiation and sensible heat. Latent heat fluxes increase in January because of largest wind speeds. The sign of the seasonal variations in latent heat flux agree with results from Stearns and Weidner (1993). The amplitude of monthly fluxes is up to an order of magnitude greater than Antarctic estimates.

Relative humidity *(RH)* is compared with elevation. This reveals decreasing moisture away from the coasts, typical of hygric continentality (Fig. 3.6). Relative humidity observations are lowest in winter and greatest in summer, conforming with climatological variations of water vapor in the Arctic (Serreze et al., 1995). There is a decrease of relative humidity with increasing elevation despite the fact that the air temperature decreases with elevation, an effect that would increase RH as the dew-point depression decreases. This pattern is least apparent in summer, possibly because there is less of a temperature gradient from the ice margin to the summit and melt conditions provide more moisture. The largest elevation gradient in the relative humidity occurs in fall because melt is persisting at lower elevations and refreeze has begun at the higher

elevations. Minimal relative humidity at high elevations will contribute to an increase in sublimation because of greater water vapor diffusivity.

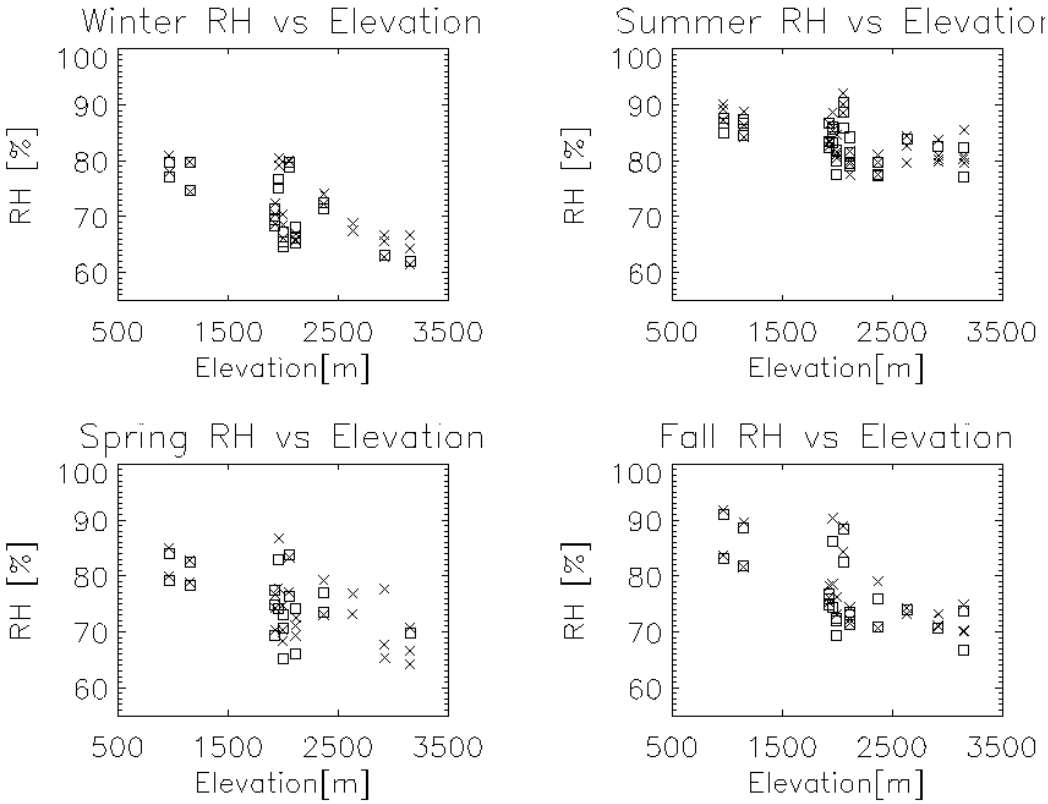

Figure 3.6: Monthly mean values of relative humidity grouped by season and plotted against elevation. Each of two profile measurements is featured. The square (cross) represents the upper (lower) level on the profile.

3.4 Comparison of Mass Flux Calculations to Accumulation Rates

Where available, the annual sum of hourly evaporative mass flux is compared with the average accumulation rate from PARCA ice cores (Table 3.2).

The absolute ratio of sublimation to accumulation rate ranges from 0.01 to 1.6. These figures require explanation in light of the complex regional climate variations on the Greenland ice sheet. At the Summit of Greenland, sublimation may cause a reduction of accumulation potential by 45%. This result seems reasonable since sublimation rates can increase with decreasing elevation (Schmidt, 1972) due to lower barometric pressure and its effect on lower air viscosity. Undersaturation of the air is also greatest near Greenland's summit (Fig. 3.7).

In north Greenland, where accumulation rates tend to be small (< 15 cm water equivalent per year), more than 1.5 times the remaining accumulation amount may sublimate. This result makes intuitive sense with GC-Net AWS surface height records that show numerous snow accumulations that return to the pre-snowfall height under high wind conditions (Fig. 3.7).

Table 3.2 Comparison of Annual Sublimation Estimates with Accumulation Rates

Station	Sublimation [cm yr^{-1}]	Accumulation [cm yr^{-1}]	Sublimation / Accumulation
Crawford Pt.	1996: -9 1997: -2	48	0.18 0.04
NASA-U	1997: -17	34	0.51
GITS	1996 : 0	34	0.01
Humboldt	1996 : -22 1997: -16	14	1.60 1.17
Summit	1997: -11	24	0.45
TUNU-N	1997: -15	10	1.5
DYE-2	1997: -7	33	0.22
JAR	1997: -58	-100	0.58
Saddle	1997: 24	45	0.53
NASA-E	1997: -13	14	0.93
CP-2	1997: -15	48, 62	0.32, 0.24

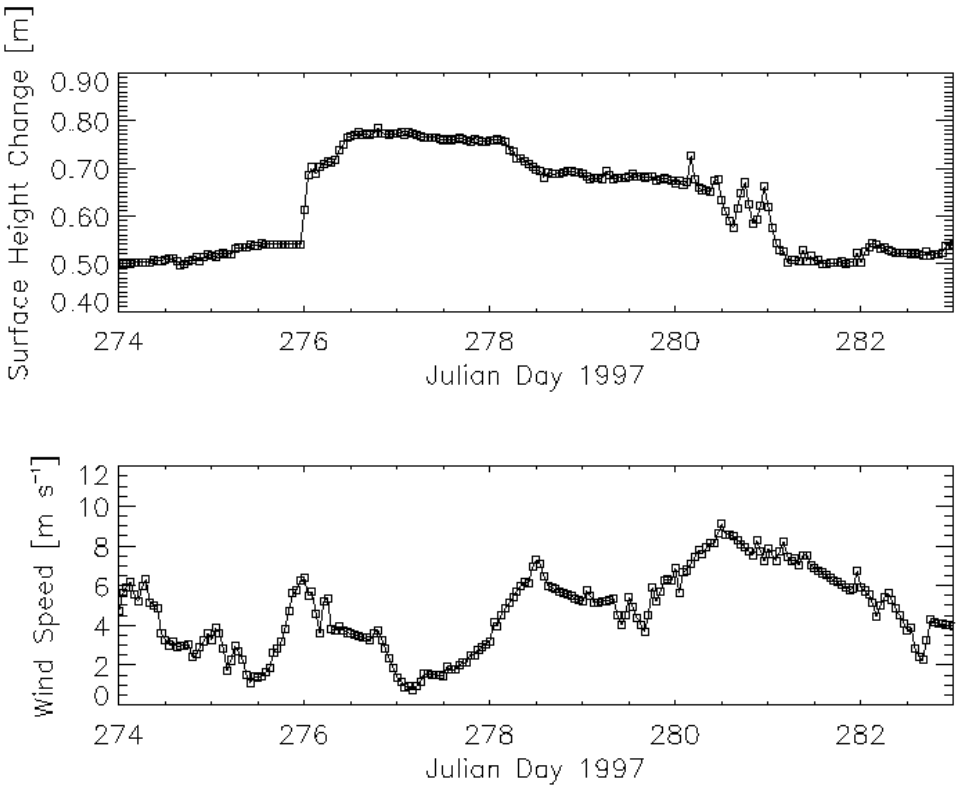

Figure 3.7: (Top) surface height variations at the TUNU-N AWS indicating loss of accumulation. (Bottom) wind speed record with peaks that correspond well with surface height reductions in top top graph.

In the ablation zone, 58% of the annual ablation is calculated to occur as a result of sublimation. The large sublimation rates at lower elevations result from warmer temperatures, lower surface albedo, and maximum wind speeds. Larger positive net radiation gives a source of sensible heat to drive sublimation.

At the Saddle, the aerodynamic profile method predicts that over half of the remnant accumulation comes in the form of water vapor deposition. The accumulation rate at Saddle is relatively large, reflecting the largest accumulation rates in Greenland observed on the southeast slope. At GITS, the annual moisture budget seems to be in equilibrium. This is not unreasonable do to the frequent observation of frozen wind propellers and springtime human observations of ice fog. At NASA-E, as much as 90% of the potential accumulation is estimated to sublimate. The difference between Crawford Pt on an undulation crest and CP2 in an adjacent undulation basin is the opposite that is expected. The above quoted sublimation values are our first estimate based on the current AWS data, and they will be revised in the near future.

3.5 Blowing Snow Mass Fluxes

Results from Pomeroy and Gray (1993) seem to provide the most accurate blowing snow mass flux (Q) parameterization.

$$Q = 2.1796x10^{-6}U_{10m}^{\ 4.04}$$

Q is in units of mass transported across an orthogonal unit length per unit time [kg m^{-1} sec^{-1}] given wind speed at 10 m simulated from GC-NET data. Annual fluxes for AWS sites in Greenland are given in units of terra (10^{12}) grams per kilometer cross section per year. The model represents snow availability using and empirical fit of observed blowing snow entrainment thresholds (U_T) with 10-m wind speeds and air temperature (Li and Pomeroy 1997).

$$U_T(10m) = 9.43 + 0.18T + 0.0033T^2$$

T is in Celsius units. No blowing snow for air temperatures above 0° C is assumed. The observed correlation of blowing snow flux and elevation was exploited as an estimate of the blowing snow mass flux at all elevations on the ice sheet (Fig. 3.8).

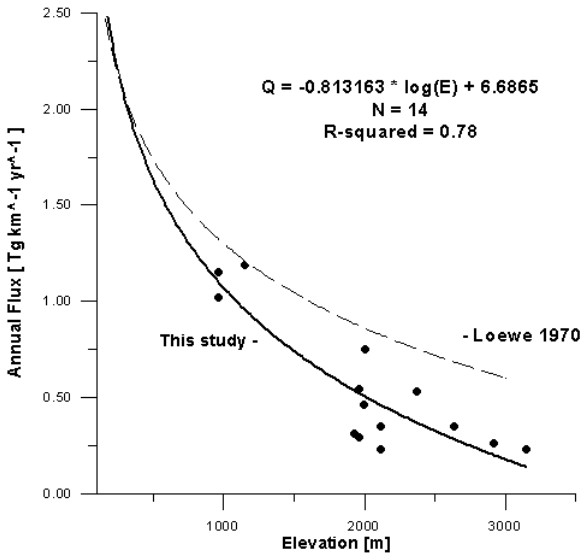

Figure 3.8: Relationship between blowing snow mass flux and elevation.

Largest blowing snow mass fluxes were found at the lower elevations of the Greenland ice sheet due to strongest katabatic wind speeds at low elevations. This result also illustrates the need for observations near the ice margin at lower elevations. The map of annual flux reflects the larger elevation gradient along the ice margin (Fig. 3.9). Wind direction vectors for Greenland were constructed using GC-Net data and model results from Bromwich (1996).

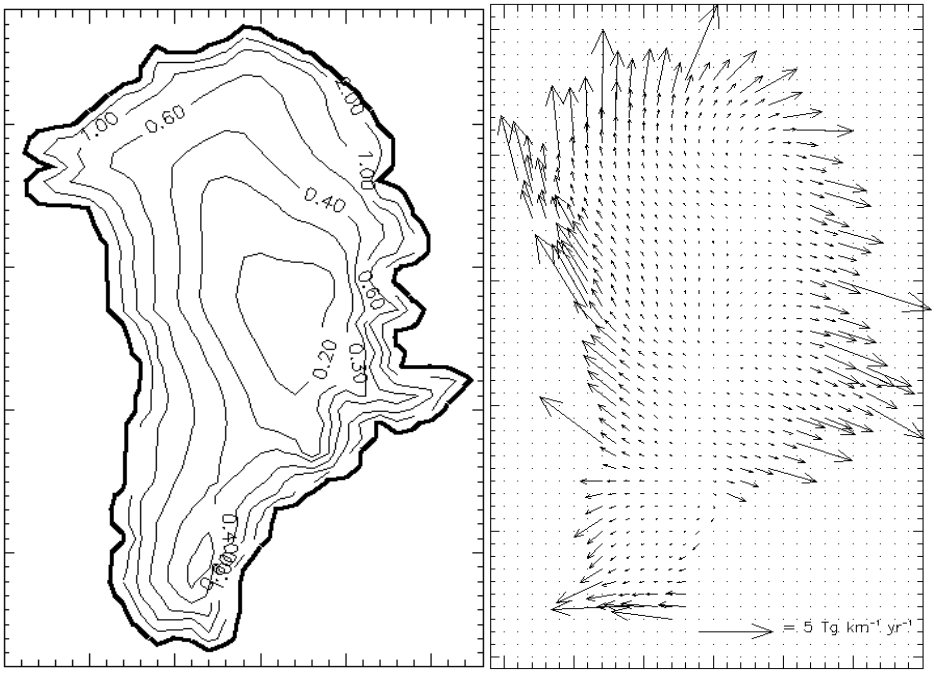

Figure 3.9: (Left plot) *Estimates for blowing snow mass flux for the Greenland ice sheet [Terra g km^{-1} yr^{-1}].* (Right plot) *Annual estimated vectors of blowing snow transport.*

Blowing snow is important to local-scale mass balance even while mass loss off the ice-sheet edge is small. The lower elevations are most prone to the effects of blowing snow, where increased wind speed ensure larger snow transport magnitudes and larger ventilation factors leading to increased sublimation rates. Although, high elevation sites are also susceptible due to increased sublimation from larger incoming solar radiation fluxes and larger water vapor diffusivity. Ultimately, the local-scale effects must contribute to the mass balance of the ice sheets on a whole. Modulation of sublimation amounts by inter-annual variability in windiness may be the most important factor since much of redistributed snow is sublimed. Further study may be concerned with the analysis of any long-term wind speed records from Greenland.

3.6 Wind Speed and Directional Frequencies

Due to the 4th power dependence of snow transport on wind speed, a less frequent higher wind speed from a less common direction can dominate the transport vector. The azimuthal distribution of wind speed as a function of wind speed is an important factor in determining the net transport vector. For example, at the Swiss Camp the largest potential blowing snow fluxes are from 10° counterclockwise of the prevailing wind direction (Table 3.3). Assuming a 10-m wind speed entrainment threshold of 7.5 m/s, potential blowing snow transport is calculated (Table 3.4).

Table 3.3: Distribution of wind speed frequency (%) by Class: Swiss Camp

Wind Speed Classes [m/s]

Azimuth	0.- 3.	3.- 6.	6.- 9.	9.-12.	12.-15.	15.-18.	18.-21.	21.-24.	24.-27.	27.-30.	Totals
0 10	0.07	0.00	0.00	0.00	0.00	0.00	0.00	0.00	0.00	0.00	0.077
10 20	0.11	0.03	0.00	0.00	0.00	0.00	0.00	0.00	0.00	0.00	0.140
20 30	0.11	0.08	0.00	0.00	0.00	0.00	0.00	0.00	0.00	0.00	0.200
30 40	0.17	0.05	0.00	0.00	0.01	0.00	0.00	0.00	0.00	0.00	0.228
40 50	0.16	0.08	0.00	0.01	0.00	0.00	0.00	0.00	0.00	0.00	0.246
50 60	0.14	0.08	0.00	0.00	0.01	0.00	0.00	0.00	0.00	0.00	0.239
60 70	0.15	0.09	0.01	0.01	0.00	0.00	0.00	0.00	0.00	0.00	0.267
70 80	0.24	0.34	0.11	0.03	0.02	0.00	0.00	0.00	0.00	0.00	0.737
80 90	0.36	1.54	0.59	0.21	0.04	0.14	0.04	0.00	0.00	0.00	2.929
90 100	0.53	1.88	2.45	1.84	0.68	0.49	0.08	0.03	0.01	0.01	8.004
100 110	0.61	1.70	2.97	3.13	1.09	0.49	0.13	0.08	**0.05**	0.01	10.260
110 120	0.54	1.84	4.61	**4.53**	**1.66**	**0.82**	0.28	0.06	0.02	0.01	14.370
120 130	*0.58*	*3.25*	***6.44***	*4.50*	*1.27*	*0.61*	***0.32***	*0.08*	*0.02*	*0.01*	***17.075***
130 140	0.78	**4.45**	5.00	2.51	0.72	0.37	0.25	**0.12**	0.03	0.02	14.248
140 150	**0.87**	3.42	2.89	1.37	0.49	0.21	0.12	0.06	0.03	**0.04**	9.495
150 160	0.66	2.35	1.66	0.72	0.35	0.14	0.07	0.03	0.01	0.00	5.994
160 170	0.69	1.54	0.98	0.40	0.14	0.07	0.03	0.00	0.02	0.00	3.883
170 180	0.51	1.17	0.73	0.27	0.09	0.03	0.01	0.01	0.00	0.00	2.838
180 190	0.43	1.01	0.58	0.19	0.09	0.03	0.02	0.00	0.01	0.00	2.368
190 200	0.35	0.65	0.45	0.15	0.07	0.04	0.01	0.00	0.00	0.01	1.733
200 210	0.34	0.45	0.18	0.13	0.05	0.02	0.02	0.00	0.00	0.00	1.182
210 220	0.20	0.20	0.13	0.09	0.04	0.02	0.00	0.00	0.00	0.00	0.687
220 230	0.16	0.14	0.06	0.04	0.03	0.01	0.00	0.00	0.00	0.00	0.452
230 240	0.19	0.12	0.05	0.01	0.02	0.01	0.00	0.00	0.00	0.00	0.393
240 250	0.18	0.07	0.03	0.02	0.00	0.00	0.00	0.00	0.00	0.00	0.302
250 260	0.13	0.06	0.01	0.02	0.00	0.00	0.00	0.00	0.00	0.00	0.228
260 270	0.15	0.04	0.01	0.00	0.00	0.00	0.00	0.00	0.00	0.00	0.203
270 280	0.09	0.05	0.00	0.00	0.00	0.00	0.00	0.00	0.00	0.00	0.140
280 290	0.09	0.07	0.00	0.00	0.00	0.00	0.00	0.00	0.00	0.00	0.168
290 300	0.06	0.06	0.02	0.00	0.00	0.00	0.00	0.00	0.00	0.00	0.144
300 310	0.10	0.06	0.01	0.00	0.00	0.00	0.00	0.00	0.00	0.00	0.165
310 320	0.05	0.04	0.00	0.00	0.00	0.00	0.00	0.00	0.00	0.00	0.098
320 330	0.10	0.05	0.00	0.00	0.00	0.00	0.00	0.00	0.00	0.00	0.165
330 340	0.11	0.05	0.00	0.00	0.00	0.00	0.00	0.00	0.00	0.00	0.158
340 350	0.05	0.06	0.02	0.00	0.00	0.00	0.00	0.00	0.00	0.00	0.123
350 360	0.02	0.05	0.00	0.00	0.00	0.00	0.00	0.00	0.00	0.00	0.063
Totals	**10.06**	**27.12**	**29.99**	**20.20**	**6.89**	**3.50**	**1.39**	**0.49**	**0.23**	**0.12**	**100.000**

Table 3.4: Distribution of Potential Snow Transport [metric tons / m] by Class: Swiss Camp

Wind Speed Classes [m/s]

Azimuth	0.- 3.	3.- 6.	6.- 9.	9.-12.	12.-15.	15.-18.	18.-21.	21.-24.	24.-27.	27.-30.	Totals
0 10	0.00	0.00	0.00	0.00	0.00	0.00	0.00	0.00	0.00	0.00	0.000
10 20	0.00	0.00	0.00	0.20	0.00	0.00	0.00	0.00	0.00	0.00	0.204
20 30	0.00	0.00	0.00	0.20	0.00	0.00	0.00	0.00	0.00	0.00	0.204
30 40	0.00	0.00	0.00	0.00	0.95	0.00	0.00	0.00	0.00	0.00	0.954
40 50	0.00	0.00	0.00	0.41	0.00	0.00	0.00	0.00	0.00	0.00	0.409
50 60	0.00	0.00	0.07	0.00	1.43	0.00	0.00	0.00	0.00	0.00	1.500
60 70	0.00	0.00	0.21	0.61	0.48	0.00	0.00	0.00	0.00	0.00	1.296
70 80	0.00	0.00	2.12	1.63	2.39	0.95	1.71	0.00	0.00	0.00	8.811
80 90	0.00	0.00	11.57	12.26	5.73	39.11	17.14	2.85	0.00	0.00	88.657
90 100	0.00	0.00	47.87	107.08	93.04	133.55	39.41	22.77	13.36	26.58	483.680
100 110	0.00	0.00	58.01	182.08	148.87	133.55	61.69	65.47	66.80	13.29	729.760
110 120	*0.00*	*0.00*	*89.93*	*264.03*	*225.21*	*222.27*	*138.81*	*48.39*	*31.17*	*26.58*	***1046.384***
120 130	0.00	0.00	125.74	262.39	173.20	165.99	157.66	62.62	22.27	13.29	983.161
130 140	0.00	0.00	97.66	146.11	98.29	101.12	121.67	99.62	35.63	33.23	733.338
140 150	0.00	0.00	56.50	79.70	66.80	57.24	58.26	45.54	40.08	73.11	477.229
150 160	0.00	0.00	32.39	42.10	48.19	38.16	32.56	25.62	17.81	6.65	243.477
160 170	0.00	0.00	19.11	23.50	19.56	20.03	13.71	2.85	31.17	0.00	129.933
170 180	0.00	0.00	14.18	15.94	12.41	7.63	6.85	11.39	4.45	6.65	79.493
180 190	0.00	0.00	11.23	11.24	12.88	7.63	10.28	0.00	8.91	6.65	68.820
190 200	0.00	0.00	8.77	8.99	9.07	9.54	5.14	2.85	4.45	13.29	62.096
200 210	0.00	0.00	3.49	7.77	6.20	4.77	8.57	2.85	0.00	0.00	33.646
210 220	0.00	0.00	2.47	5.11	5.25	5.72	0.00	2.85	4.45	0.00	25.846
220 230	0.00	0.00	1.16	2.04	4.29	2.86	1.71	2.85	4.45	6.65	26.023
230 240	0.00	0.00	1.03	0.61	2.39	1.91	0.00	0.00	0.00	0.00	5.934
240 250	0.00	0.00	0.55	1.23	0.00	0.95	1.71	0.00	0.00	0.00	4.442
250 260	0.00	0.00	0.21	1.02	0.48	0.00	0.00	0.00	0.00	0.00	1.704
260 270	0.00	0.00	0.27	0.20	0.00	0.00	0.00	0.00	0.00	0.00	0.478
270 280	0.00	0.00	0.00	0.00	0.00	0.00	0.00	0.00	0.00	0.00	0.000
280 290	0.00	0.00	0.07	0.20	0.00	0.00	0.00	0.00	0.00	0.00	0.273
290 300	0.00	0.00	0.41	0.20	0.00	0.00	0.00	0.00	0.00	0.00	0.615
300 310	0.00	0.00	0.14	0.00	0.00	0.00	1.71	0.00	0.00	0.00	1.851
310 320	0.00	0.00	0.07	0.00	0.00	0.00	0.00	0.00	0.00	0.00	0.068
320 330	0.00	0.00	0.07	0.00	0.00	0.00	0.00	0.00	4.45	6.65	11.168
330 340	0.00	0.00	0.00	0.00	0.00	0.00	0.00	0.00	0.00	0.00	0.000
340 350	0.00	0.00	0.34	0.00	0.00	0.00	0.00	0.00	0.00	0.00	0.342
350 360	0.00	0.00	0.00	0.00	0.00	0.00	0.00	0.00	0.00	0.00	0.000

Totals 0.00 0.00 585.64 1176.88 937.09 953.01 678.61 398.50 289.46 232.61 5251.72

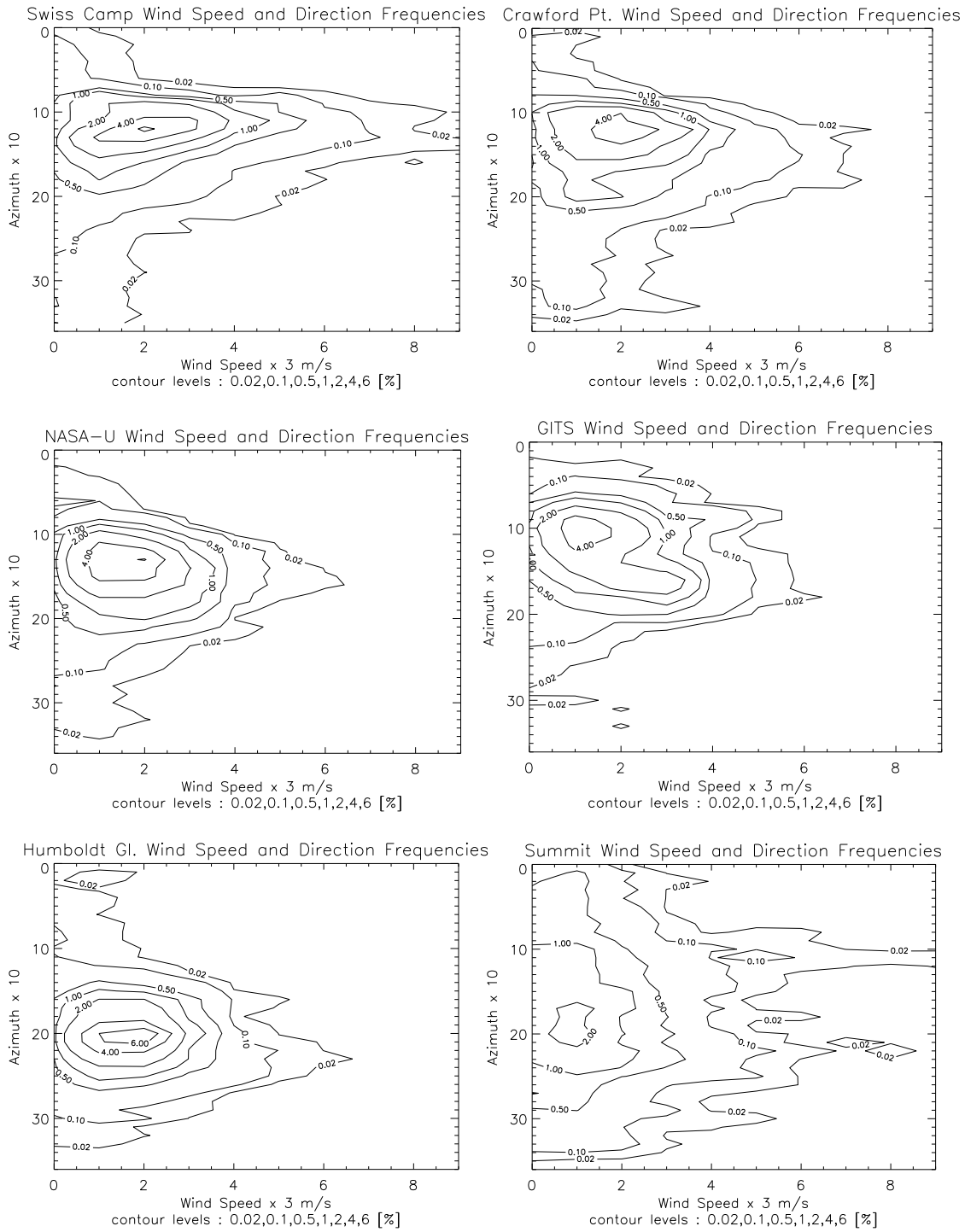

Figure 3.10: Frequency contour plot of wind direction and speed for the Swiss Camp, Crawford Point-1, NASA-U, GITS, Humboldt Glacier, and Summit AWS locations

3.7 Increased UV-Radiation over the Greenland Ice Sheet

Enhanced UV cloud transmission was measured over snow surfaces at the Swiss Camp. Cloud attenuation of total radiation is twice that of UV radiation, whereas in mid-latitudes the attenuation ration is 1.2. Consequently, higher UV cloud transmission over large snow covered surfaces will expose individuals at a higher UV risk.

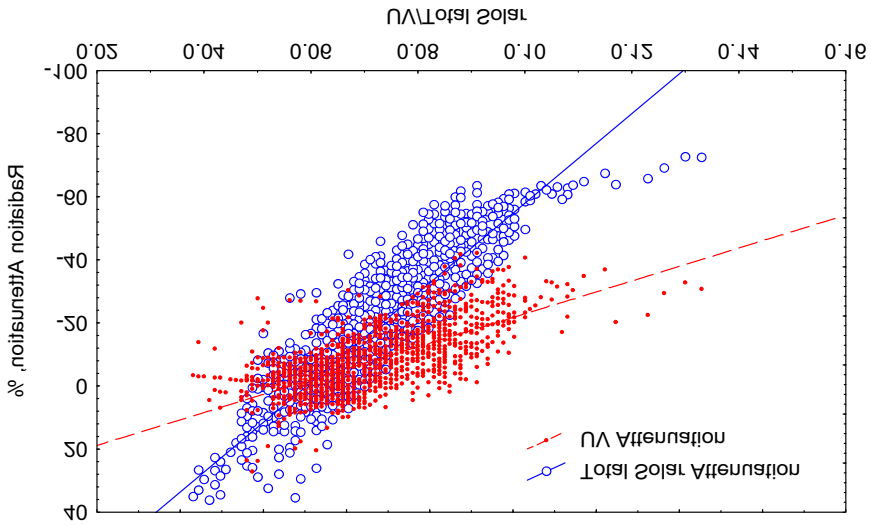

Figure 3.11: Attenuation of total solar and UV radiation as a function of the UV to total solar radiation ratio. A positive attenuation indicates a radiation enhancement above clear skies due to.clouds.

3.8 Faceted Crystal Growth due to Katabatic Storm Events

Faceted snow crystals were found under wind crusts at the Tunu-N location (Fig. 2.1). These crusts appear to originate during winter. Snow and air temperatures from the Tunu-N AWS suggest that the katabatic storms are responsible for the wind crust and the faceted layers. The approximated temperature gradients for the top snow cover (5-14 cm in depth) show values in excess of 50 K m^{-1} (a 5 K gradient over 10 cm) for periods of high wind (Fig. 3.12). The gradient even exceeds 100 K m^{-1} on Nov. 11, 1996, assuming a 3-4 K error in snow surface temperature approximation (colder snow surface during low wind). Also large negative temperature gradients in excess of 100º K m^{-1} were found to be caused by atmospheric warming during katabatic storms, resulting in a reversal of the water vapor flux. The snow temperature at 1 m depth varied only by ±1º C over the period of 8 days shown in Figure 3.12, hence large temperature gradients (negative as well as positive) are limited to the top snow layer. This simple approximation suggests that snow temperature gradients in excess of the critical gradient (~25 K m^{-1}) necessary for faceted crystal development can occur during katabatic storms, and after the storms with subsequent radiative cooling. In addition to its climatological significance in the snow record, understanding the formation of these layers is especially important to the interpretation of microwave satellite observations of firn.

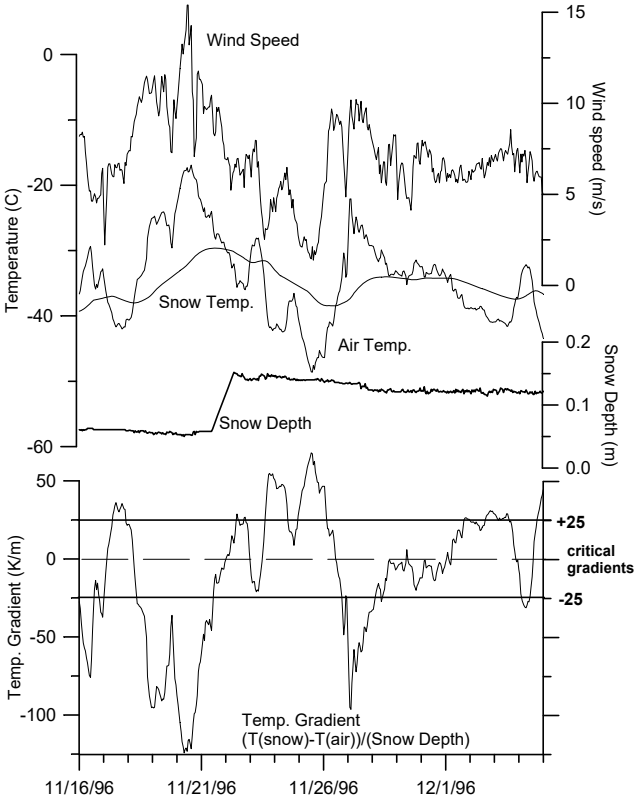

Figure 3.12: Hourly automatic weather station record of wind speed, air and snow temperatures, and snow height for Tunu-N in north-east Greenland (Fig. 2.1). The zero level for the snow height represents the summer 1996 height, and the position of the first snow temperature thermistor. The temperature gradient in the top snow layer exceeds the critical value of 25 K m^{-1} necessary for faceted crystal development several times

3.9 References

Bromwich, D. H., Y. Du, and K. M. Hines, Wintertime Surface Winds over the Greenland Ice Sheet, Mon. Wea. Rev., 124, 1941-1947, 1996.

Li, L. and J. W. Pomeroy, Estimates of Threshold Wind Speeds for Snow Transport Using Meteorological Data, *J. Appl. Met.*, 36(3), 205-213, 1997.

Loewe, F.,Transport of Snow on Ice Sheets by the Wind, *Studies On Drifting Snow*, Melbourne University, Meteorology Dept. Pub. 13, 69 pp., 1970.

Pomeroy, J. W, Gray, D. M, The Prairie Blowing Snow Model: Characteristics, Validation, Operation. J. Hydrology, 144, 165-192, 1993.

Serreze, M. C., M. C. Rehder, R. G. Barry, J. D. Kahl, and N. A. Zaitseva, The distribution and transport of atmospheric water vapor over the Arctic, *Int. J. Climatol.*, Vol. 15, pp. 709-727, 1995.

Schmidt, R. A, Sublimation of Wind Transported Snow - A Model, USDA Forest Service Research Paper RM-90, Rocky Mountain Forest and Range, 24 pp., 1972.

Stearns C. R. and G. A. Weidner, Sensible and Latent Heat Flux Estimates in Antarctica, In Antarctic Meteorology and Climatology: Studies Based on Automatic Weather Stations, Antarctic Research Series, Vol. 61, pp. 109-138, 1993.

4.0 Proposed Field Work 1999

4.1 AWS Maintenance, and Swiss Camp Experiments

- Any station that is revisited next field season will be converted to a new mast design that will allow more timely extension. Further, re-calibration of all sensors, net radiometer servicing, and leveling of all radiometers will be done. In addition, snow pit data will be collected.
- New AWS stations to represent low elevation climate as part of elevation transect (JAR region) and at the east coast where major thickness changes have been observed.
- Additional SE station to fill data gap around 72° N along the eastern side of Greenland (former location Tunu-S)
- NASA/GSFC Lidar installation for monitoring aerosol and clouds on an annual basis at the Swiss Camp
- Atmospheric kite experiment: profile measurements of temperature, humidity, radiation and aerosol concentration in the first 1-2 km to study the boundary layer structure during katabatic storm events.
- Ground-penetrating radar transect between Swiss Camp and Crawford Point to monitor layering in the firn.

Priority list of AWS maintenance

Site	*Tasks*	*Time on Site Needed*	*Priority*
GITS	Extension. New Transmitter. Firn Temperature String.	2-3 days	High
NASA-U	Extension. New Transmitter. New Firn Temperature String.	2-3 days	High
Saddle	Extension. Transmission reset 1998 did not work.	2-3 days	High
NASA-SE	Extension. Transmitter.	1-3 days	High
SDOME	Extension. 1 x T/RH broken.	2-3 days	High
JAR	New tower foundation. TC Air out.	1* day	High
CP 1 and 2	Extend one tower	2* days	Medium
Swiss Camp	Reset transmission .	2* days	
Summit	Extension.	2-3 days	Medium
NASA-E	1 x T/RH broken	1 day	Medium
Humboldt	Not Visited since 1996. 2 x T/RH broken	1 day	Medium
Tunu-N	Might be something in way of wind direction sensors or a processing problem. more noisy firn TC measurements after 1998 visit?	2-3 hours	low

- - to be performed as part of Swiss Camp traverse work

4.2 Proposed Budget for New AWS Stations and Upgrades

1 AWS AWS on glacier tongue (300 m amsl) in East Greenland to measure glacier climate and mass balance in ablation region where airborne laser showed largest decrease	*$18,000*
1 AWS AWS in SE Greenland (Tunu-S: 69.7 N, 33 E) to close data gap between 67.5 and 75 N	*$ 18,000*
1 AWS AWS on glacier tongue (300 m amsl) in the Jakobshavn area to complete transect from Summit - Crawford Point - Swiss Camp – Jar. This glacier station in the W will be compliment to the new station in the E.	*$ 18,000*
30 T/H upgrade ($425 each) Upgrade temperature humidity sensors with ventilated sensors Most of the current T/H sensors break after 2 years, and they have a radiation error. The new sensors are ventilated (during solar days, powered by solar cell)	*$ 12,750*
Tower upgrades The AWS towers in the south and the west where accumulation is large need to be extended every season. We have designed a new tower which can be extended within an hours, Which would reduced the logistic cost in future for the AWS maintenance. We do not replace The old towers, but will modify them.	*$ 5,000*
Total	$71,750

Remarks:
The data transmission for the 3 additional AWS will be paid by NOAA, since our Institute (CIRES) will not be charged for GOES transmission (NOAA/CU Coop. Inst.)

5.0 Publications Supported from this Grant

Abdalati, W., and K. Steffen, Snowmelt on the Greenland ice sheet as derived from passive microwave satellite data, J. Climate, 10(2), 165-175, 1997.

Abdalati, W., and K. Steffen, The apparent effects of the Mt. Pinatubo eruption on the Greenland ice sheet melt extent, Geophys. Res. Lett., 24(14), 1795-1797, 1997.

Abdalati, W., K. Steffen, Accumulation and hoar effects on microwave emission on the Greenland ice sheet dry snow zones, J. Glaciology (in press).

Anklin, M., R.C. Bales. E. Mosley-Thompson, and K. Steffen, Annual accumulation at two sites in northwestern Greenland during recent centuries, J. Geophys. Res., (in press)

Box, J., and K. Steffen, An empirically based model for estimating blowing snow mass fluxes for the Greenland Ice Sheet, 5th Int. Conf. Polar Met. and Oceanogr., Dallas Jan 10-15 1999, 79 Annual Amer. Met. Soc. General Meeting, paper 12.7, 1999.

Serreze, M., J. Key, J. Box, J. Maslanik, and K. Steffen, A new monthly climatology of global radiation for the Arctic and comparison with NCEP-NCAR reanalysis and ISCCP-C2 field, J. Climate, 11, 121-136, 1998.

Steffen, K., Effect of solar zenith angle on snow aniosotropic reflectance, IRS '96: Current Problems in Atmospheric Radiation, Smith and Stamnes (Eds), Deepak Publishing, 41-44, 1997.

Steffen, K., W. Abdalati, and I. Seherjal, Faceted crystal formation on NE-Greenland low accumulation region, J. Glaciology (in press).

Steffen, K., and J. Box, Recent climate variability of the Greenland ice sheet: first results from the Greenland climate network, 5th Int. Conf. Polar Met. and Oceanogr., Dallas Jan 10-15 1999, 79 Annual Amer. Met. Soc. General Meeting, paper 4.6, 1999.

Stroeve, J., M. Haefliger, and K. Steffen, Surface temperature fro ERS-1 ATSR infrared thermal satellite data in Polar regions, J. Appl. Meteorol., 35(8), 1231-1239, 1996.

Strove, J., Anne Nolin, and K. Steffen, Comparison of AVHRR-derived and in situ surface albedo over the Greenland ice sheet, Remote Sens. Environ., 62, 262-276, 1997.

Stroeve, J., and K. Steffen, Variability of AVHRR-derived clear-sky surface temperature over the Greenland ice sheet, J. Appl. Meteorol., 37, 23-31, 1998.

Stroeve, J., and A. Nolin, The changing albedo of the Greenland ice sheet: implications for climate modeling, Ann. of Glaciol. 25, 51-57, 1997.

6.0 Budget